HAL
open science

Towards a new concept for high sensitivity Compton scatter emission imaging

M. K. Nguyen, C. Driol, T. T. Truong

To cite this version:

M. K. Nguyen, C. Driol, T. T. Truong. Towards a new concept for high sensitivity Compton scatter emission imaging. Journal of the European Optical Society : Rapid publications, 2008, pp.08010. 10.2971/jeos.2008.08010 . hal-00672246

HAL Id: hal-00672246

https://hal.science/hal-00672246v1

Submitted on 20 Feb 2012

HAL is a multi-disciplinary open access archive for the deposit and dissemination of scientific research documents, whether they are published or not. The documents may come from teaching and research institutions in France or abroad, or from public or private research centers.

L'archive ouverte pluridisciplinaire **HAL**, est destinée au dépôt et à la diffusion de documents scientifiques de niveau recherche, publiés ou non, émanant des établissements d'enseignement et de recherche français ou étrangers, des laboratoires publics ou privés.

NEW CONCEPT FOR HIGH SENSITIVITY SCATTERED GAMMA-RAY IMAGING

M. K. Nguyen[1], *Clémence Driol*[2], *T. T. Truong*[2]

[1] ETIS / CNRS UMR 8051 / ENSEA / Université de Cergy-Pontoise
6 avenue du Ponceau, 95014 Cergy-Pontoise Cedex, France
[2]LPTM / CNRS UMR 8089 / Université de Cergy-Pontoise
2 rue Adolphe Chauvin, 95302 Cergy-Pontoise Cedex, France
e-mails: truong@u-cergy.fr, mai.nguyen-verger@u-cergy.fr

ABSTRACT

A new efficient scheme for imaging gamma-ray emitting objects is advocated in this work. A few years back we have put forward the idea of collecting data on Compton scattered rays to reconstruct an object in three dimensions and shown how it works with a collimated detector. To increase drastically the sensitivity of this modality as well as its field of view and resolution we propose now that data acquisition should be performed without collimation. We discuss image formation by scattered radiation in this context by computing and comparing the related Point Spread Functions (PSF) and comment on their properties. We also present numerical simulations to support the attractiveness of this modality.

Key words: Gamma-ray imaging, sensitivity, photon Compton scattering, image formation, object reconstruction.

1. INTRODUCTION

Emission imaging with gamma rays is widely used in numerous fields such as medical imaging, non-destructive testing, gamma astronomy and environmental survey. In conventional nuclear imaging, a collimated gamma camera rotates in space to collect primary radiation emitted by an object under investigation. In this case Compton scatter radiation behaves generally as noise hindering image quality and consequently correction to scatter should be applied.

However recently an interesting new imaging concept, which precisely uses, as imaging agent, scattered radiation by the object medium (instead of primary radiation), has been proposed. A spatially fixed collimated gamma camera records now images labeled by the energy of scattered radiation (or equivalently its scattering angle). It is then shown that the reconstruction of a three-dimensional object is feasible using this data [1, 2, 3]. However in this situation, the image sensitivity is considerably affected due to the presence of the collimator. Only about one out of 10^4 scattered photons reaches the detector. Therefore in order to record a much larger amount of scattered radiation, we propose to extend the working principle of this gamma-ray imaging to a functioning modality without collimator, as depicted by Fig. 1. However, as can be seen, this procedure differs from other proposals on scattered radiation imaging processes [4, 5, 6, 7], in particular:

- Compton tomography [8], which reconstructs the electron density of the object (instead of its activity density), and uses a moving point-like detector collecting scattered radiation from an external radiation source,

- Compton camera [9], which reconstructs the activity density of an object from scattered radiation using coincidence measurements between a site on a scatter layer-detector and another site on an absorption-detector.

As the true three-dimensional problem implies involved space geometry of scattered rays, we shall first study its two-dimensional counterpart to test the viability of this idea. To this end, we give a careful analysis of the image formation. The corresponding PSF is derived and shall be compared with the previous case where a collimator is present. Next we perform numerical reconstruction of the object radiation activity from simulated scattered radiation (recorded by a camera without collimator) to illustrate the working of this concept.

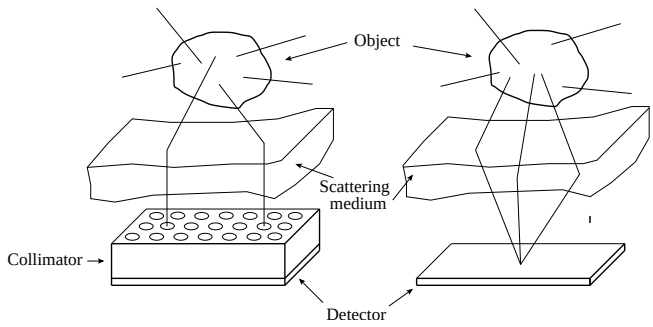

Fig. 1. Two modalities in emission scattered radiation imaging.

2. IMAGE FORMATION

To understand image formation by scattered radiation, we follow radiation propagation in a two-dimensional (2D) slice (or thin section) of a scattering medium with an electronic density n_e assumed to be approximately constant. This can be in principle implemented with a slit placed above a detector without collimator, see Fig. 2. Moreover, to concentrate chiefly on scattering effects radiation, attenuation will be left out as working hypothesis.

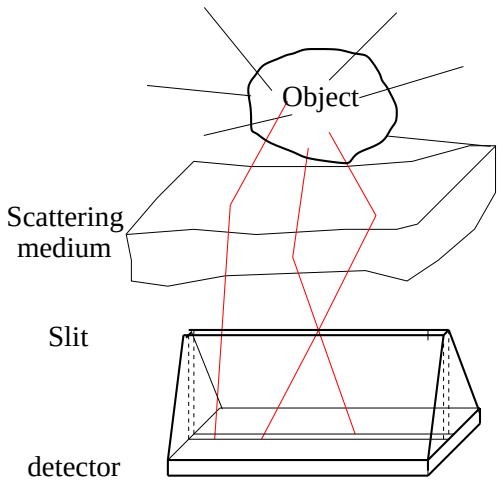

Fig. 2. Two dimensional working with a slit.

Let
- $\mathbf{S} = (x_S, y_S)$ be a radiation emitting point source of an object described by its activity density $f(\mathbf{S})$ (number of photons emitted per unit time isotropically in all directions,
- $\mathbf{M} = (x_M, y_M)$, a scattering site in the medium,
- $n_e(\mathbf{M})$, the electron density at site $\mathbf{M}$,
- $\mathbf{D} = (x_D, y_D)$, a detection site on a linear detector which collects the photon flux density at a photon energy E_ω (see Eq. (1)).

The energy of scattered photon is related to the scattering angle ω by the Compton relation:

$$E_\omega = E_0 \, \frac{1}{1 + \varepsilon(1 - \cos\omega)}, \tag{1}$$

where E_0 is the emitted photon energy, $\varepsilon = E_0/mc^2$ and mc^2 the rest energy of the electron.

From Fig. 3, one can see that the photon flux density reaching a site $\mathbf{M}$ is the number of photons emitted into the angular fan $d\Omega$ per unit length and per unit time:

$$\frac{f(\mathbf{S})d\mathbf{S}_S}{2\pi} \; 2\arctan\left(\frac{\sigma}{2\,|SM|}\right) \; \frac{1}{\sigma}, \tag{2}$$

where $|SM|$ is the distance between sites $\mathbf{S}$ and $\mathbf{M}$ and $d\mathbf{S}_S$ the area element around $\mathbf{S}$. The fraction of photons scattered

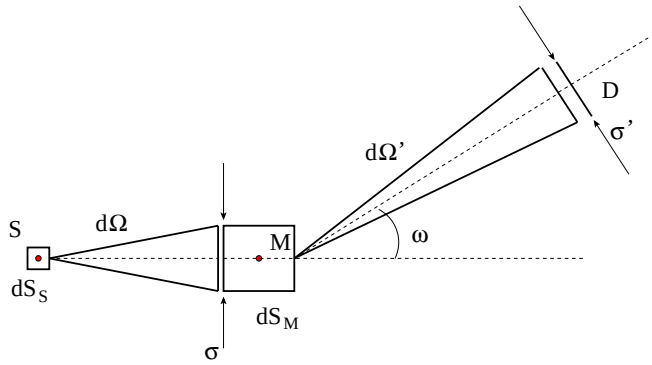

Fig. 3. Geometry of Compton scattering: source site $\mathbf{S}$, scattering site $\mathbf{M}$ and detection site $\mathbf{D}$ of width σ'.

in the direction making an angle ω with the incident direction depends on the Compton differential cross section $\sigma_S^C(\omega)$ (which has the dimension of a length in 2D) and on the number of electrons $n_e(\mathbf{M})\; d\mathbf{S}_M$ at site $\mathbf{M}$, $d\mathbf{S}_M$ being the integration area element around $\mathbf{M}$. Hence the scattering photon flux density received at the detection site $\mathbf{D}$ is given by :

$$d\phi(\mathbf{D}, \omega|\mathbf{S}) = \frac{f(\mathbf{S})d\mathbf{S}_S}{2\pi} \; 2\arctan\left(\frac{\sigma}{2\,|SM|}\right) \; \frac{1}{\sigma}$$
$$\times\, n_e(\mathbf{M})\; d\mathbf{S}_M \;\; \sigma_S^C(\omega) \;\; 2\arctan\left(\frac{\sigma'}{2\,|MD|}\right) \; \frac{1}{\sigma'} \; \cos\theta, \tag{3}$$

where θ is the angle between the outgoing photon unit vector with the detector normal unit vector, $|MD|$ the distance from scattering site $\mathbf{M}$ to detection site $\mathbf{D}$. In fact, for a given point source $\mathbf{S}$, there will be two scattering sites $\mathbf{M}_1$ et $\mathbf{M}_2$ located on two arcs of circle subtending a scattering angle $(\pi - \omega)$, as shown in Fig. 4.

The total photon flux density at a site $\mathbf{D}$ is $g(\mathbf{D}, \omega)$, the integral over all source sites and all scattering sites such that the scattering angle is ω. This last constraint is expressed by a δ-function in the integration as

$$g(\mathbf{D}, \omega) = \int\int d\phi(\mathbf{D}, \omega|\mathbf{S}) \; \delta(\widehat{SMD} - (\pi - \omega)), \tag{4}$$

where $\widehat{SMD}$ is the angle at vertex $\mathbf{M}$ of the triangle SMD (see Fig. 4). Eq. (4) describes the basic image formation process from scattered radiation measured on a detector without collimator.

3. COMPUTATION OF THE IMAGE OF A POINT SOURCE

We now compute and study the essential object in this new imaging concept: the Point Spread Function (PSF). It is, by definition, the image of a single point source at site $\mathbf{S}$. Eq. (4) can be rewritten in terms of the PSF as follows :

$$g(\mathbf{D},\omega) = \int d\mathbf{S}_S \;\; f(\mathbf{S}) \;\; PSF(\mathbf{D},\omega|\mathbf{S}). \qquad (5)$$

As shown before for a camera without collimator, the scattering sites due to a single point source $\mathbf{S}$ are located on two circular arcs subtending an angle $(\pi - \omega)$ (Eq. (4)). The photon flux density received at site $\mathbf{D}$ is then given by an integration over these two circular arcs (see Fig.4).

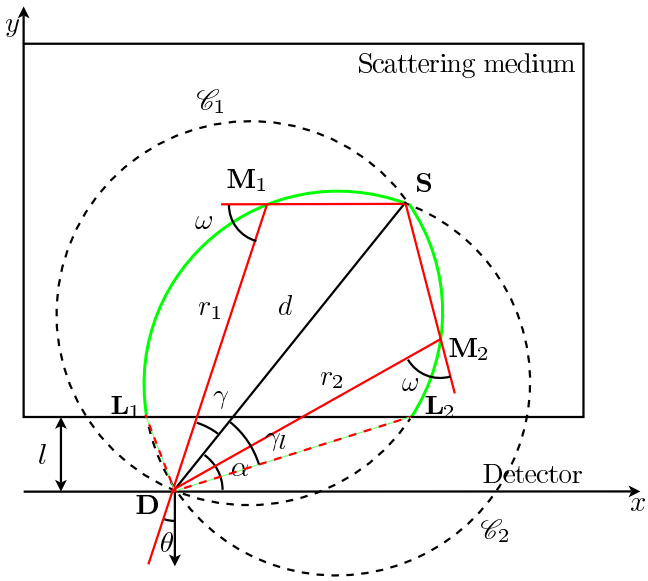

Fig. 4. Locus of scattering sites due to single point source

For computation ease, we shall assume a uniform electron density n_e and use polar coordinates (r,γ), such that $\mathbf{S} = (d,\alpha)$ with $DS = d$ and $\mathbf{M} = (r,\gamma)$, with $DM = r$ and $\overrightarrow{DM} \cdot \overrightarrow{DS} = r\, d\, \cos\gamma$.

The circular arcs have polar equations:

$$r = d\,\frac{\sin(\omega-\gamma)}{\sin\omega} \qquad \text{and} \qquad r = d\,\frac{\sin(\omega+\gamma)}{\sin\omega}, \qquad (6)$$

where γ is the angle between $\overrightarrow{DS}$ and $\overrightarrow{DM}$. The distance $|SM|$ can be extracted from a simple identity in the triangle DSM:

$$|SM| = d\,\frac{\sin\gamma}{\sin\omega}. \qquad (7)$$

And the integration area $d\mathbf{S}_M$ is now reduced to the arc element:

$$\sqrt{dr^2 + r^2 d\gamma^2} = \frac{d}{\sin\omega}\, d\gamma. \qquad (8)$$

Hence the PSF is given by the sum of the two integrations on γ:

$$PSF(\mathbf{D},\omega|\mathbf{S}) = \frac{K(\omega)\,d}{\sigma\;\sigma'\;\sin\omega} \sum_{2\text{ Arcs}} \int_0^{\gamma_l(\omega)} d\gamma\, \cos\theta(\gamma)$$

$$\arctan\left(\frac{\sigma}{2d}\frac{\sin\omega}{\sin\gamma}\right) \arctan\left(\frac{\sigma'}{2d}\frac{\sin\omega}{\sin(\omega\pm\gamma)}\right), \qquad (9)$$

where $K(\omega) = 4n_e\sigma_S^C(\omega)f_0/2\pi$, $\sigma_S^C(\omega)$ the differential Compton cross section at scattering angle ω, f_0 the intensity of the single point source and $\cos\theta = \sin(\alpha-\gamma)$ if the detector lies along the $0x$ axis and l is the distance between the line detector and the linear lower boundary of the medium L. The integration is carried out over the points inside the scattering medium. Therefore when the medium is of finite extent, the limit of the integration $\gamma_l(\omega)$, which corresponds to the intersection of the arcs of circle with the scattering medium, should be calculated beforehand, see Fig. 4.

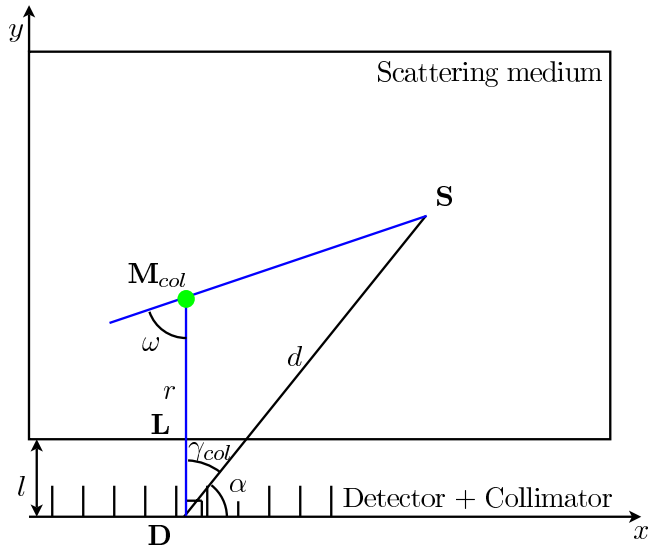

Fig. 5. Scattering site in the presence of a collimator from single point source

Now if the collimator is mounted on the detector, then only one scattering site $\mathbf{M}$, located on the perpendicular to the detector at site $\mathbf{D}$, will contribute to detection site $\mathbf{D}$, (see Fig. 5). Thus the integration on γ is restricted by a delta function which picks out only the corresponding value of γ, i.e.:

$$\gamma_{col} = \frac{\pi}{2} - \alpha. \qquad (10)$$

The resulting PSF expression for a collimated detector is:

$$PSF_{col}(\mathbf{D},\omega|\mathbf{S}) = \frac{K(\omega)\,d}{\sigma\;\sigma'\;\sin\omega}$$
$$\arctan\left(\frac{dx}{2d}\frac{\sin\omega}{\cos\alpha}\right) \arctan\left(\frac{\sigma'}{2d}\frac{\sin\omega}{\pm\cos(\alpha\mp\omega)}\right). \qquad (11)$$

Now at a fixed scattering angle ω, the PSF curve as function of the detector position with collimator has a Mexican hat shape (see Fig. 6)

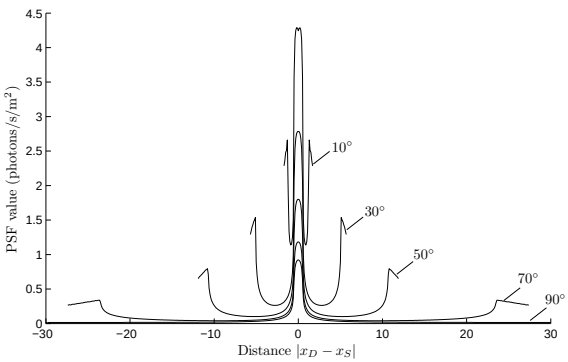

Fig. 6. PSF shapes with collimator

while the PSF curve without collimator has a wide Lorentzian shape (see Fig 7).

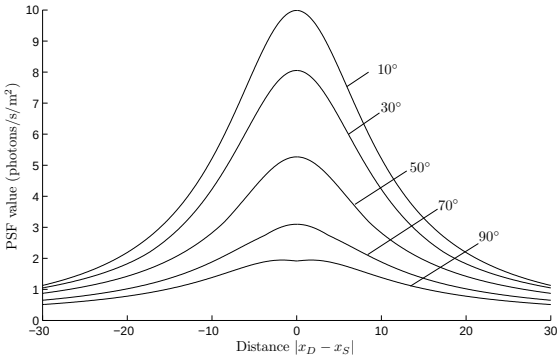

Fig. 7. PSF shapes without collimator

For example at a scattering angle of 30 degrees, Fig. 8 shows that the PSF without collimator is about 10 times stronger than the PSF with collimator.

4. NUMERICAL RECONSTRUCTION RESULTS

As an illustration of this new imaging concept, we carried out numerical reconstructions of a two-dimensional Shepp-Logan medical phantom from data computed with our model.

The 2D original object (see Fig. 9) is placed at the center of the scattering medium and a unit distance above the detector. A line detector of 55 pixels of 1 unit length, placed on

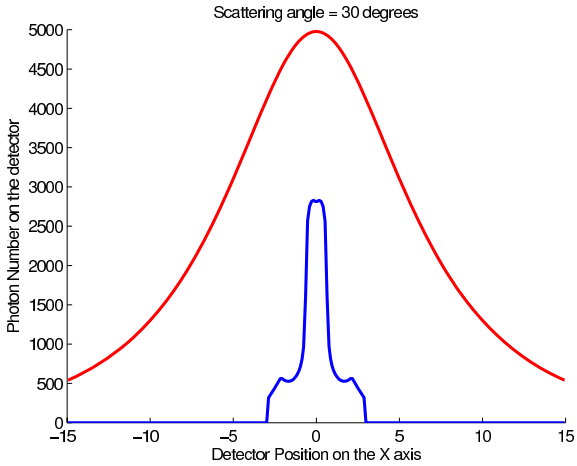

Fig. 8. Comparison of PSF with (lower blue line) and without collimator (upper red line)

the axis $y = 0$, is simulated. We consider that the scattering medium has the same properties as water. It consists of a discretized square of 55×55 elements of unit area.

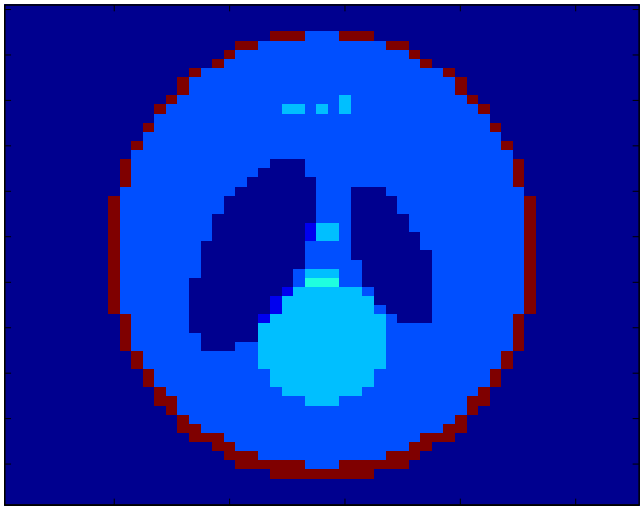

Fig. 9. Original Shepp-Logan phantom

A series of 55 images of the object corresponding to 55 different scattering angles ($12° < \omega < 132°$) have been simulated. We construct the 3025×3025 *weight matrix* by computing, for each mesh point source, the PSF at the different scattering angles for each site on the detector. The reconstruction is carried out by inverting this *weight matrix* using the Singular Value Decomposition method, which is less time

consuming, compared to other reconstruction methods.

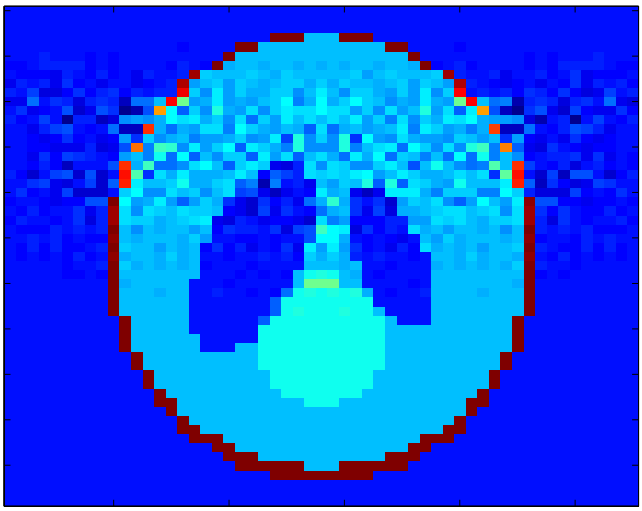

Fig. 10. Shepp-Logan phantom reconstruction with collimator

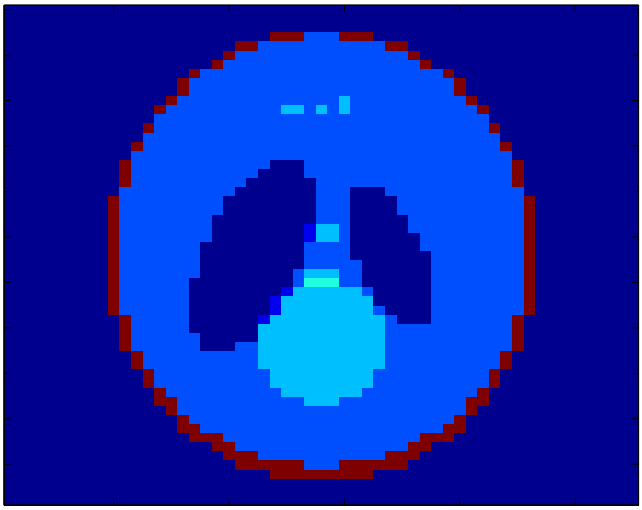

Fig. 11. Shepp-Logan phantom reconstruction without collimator

Fig. 10 and Fig. 11 show the reconstruction results with and without collimator. One observes a better agreement with the original object when the collimator is removed. In Fig. 10, we can see that the part of the object near the detector is better reconstructed than the upper part of the object. The three small structures are invisible. The reconstructive relative error is about 9.13 %. But without collimator (see Fig. 11), the whole object is correctly reconstructed. All structures are visible and the relative error is about 1.17×10^{-4} %.

These results have been subsequently validated by Montecarlo simulations [10].

5. CONCLUSION

The feasibility of image reconstruction using Compton scattered rays detected by a gamma-camera without collimator, operating in a fixed position, is demonstrated in this study. This is the essence of a new concept of high sensitivity imaging, which takes advantage of scattering rays instead of rejecting them as done usually. The main point in this imaging process by Compton scattered radiation is the fact that data acquisition is performed without the usual motion of the detector. This is a major advantage compared to existing imaging systems which require a heavy, bulky and costly mechanical rotation mechanism to move the detector around in space. Work towards an extension to three-dimensional imaging is in progress. The modeling and simulations of multiple scattered radiation in this context will be also subjects of future investigations. These promising results may open the way to new high sensitivity imaging devices which will have applications in nuclear medicine, non-destructive industrial control, high energy astrophysics, environmental survey, etc.

6. REFERENCES

[1] M.K. Nguyen and T.T. Truong, "On an integral transform and its inverse in nuclear imaging," *Inverse Problems*, vol. 18, pp. 265–277, 2002.

[2] M.K. Nguyen, T.T. Truong, H.D. Bui, and J.L. Delarbre, "A novel inverse problem in gamma-ray emission imaging," *Journal of Inverse Problems in Science and Engineering*, vol. 12, pp. 225–246, 2004.

[3] M.K. Nguyen, T. T. Truong, J. L. Delarbre, C. Roux, and H. Zaidi, "Novel approach to stationary transmission scanning using compton scattered radiation," *Phys. Med. Biol.*, vol. 52, pp. 4615–4632, 2007.

[4] R. L. Clarke, E. N. C. Milne, and G. Van Dyk, "The use of compton scattered gamma rays for tomography," *Inv. Radiology*, vol. 11, pp. 225–235, 1976.

[5] B. L. Evans, J. B. Martin, L. W. Burggaf, and M. C. Roggemann, "Nondestructive inspection using compton scatter tomography," *IEEE Transactions on Nuclear Science*, vol. 45, no. 3, June 1998.

[6] E.M.A. Hussein, "Compton scatter imaging systems," in *Bioinstrumentation: Research, Developments and Applications*, Donald L. Wise, Ed., chapter 35, pp. 1053–1086. Butterworths, 1990.

[7] P.C. Johns, R.J. Leclair, and M.P. Wismayer, "Medical x-ray imaging with scattered photons," in *Opto-Canada: SPIE Regional Meeting in Optoelectronics, Photonics and Imaging, SPIE* **TD 01**, Ottawa, Canada, May 2002, pp. 355–357.

[8] S. J. Norton, "Compton scattering tomography," *J. Appl. Phys.*, vol. 76, pp. 2007–2015, 1994.

[9] M. Singh, "An electronically collimated gamma camera for single photon emission computed tomography," *Med. Phys.*, vol. 10, pp. 421–427, 1983.

[10] C. Driol, M.K. Nguyen, and T.T. Truong, "Modelling and simulation results on high sensitivity scattered γ-ray imaging," in *Proc. 6th EUROSIM Congress on Modelling and Simulation*, Ljubljana-Slovenia, September 2007.